

Renewable chemical feedstocks from peanut shell liquefaction: Preparation and characterization of liquefied products and residue

Qinqin Zhang,¹ Guangyu Zhang,¹ Dezhi Han,² Yumin Wu¹

¹College of Chemical Engineering, Qingdao University of Science and Technology, Qingdao 266042, People's Republic of China

²Key Laboratory of Biofuels, Qingdao Institute of Bioenergy and Bioprocess Technology, Chinese Academy of Sciences, Qingdao 266101, People's Republic of China

Correspondence to: Q. Zhang (E-mail: qqzhang@qust.edu.cn)

ABSTRACT: The objective of this investigation is to liquefy peanut shell for the preparation of aromatic polyol-rich products. The influences of reaction parameters are discussed. It is found that, compared to single-solvent, the mixture of polyethylene glycol and glycerol as solvents shows higher liquefaction efficiency. And the maximum liquefaction yield of 98.7 wt % can be achieved when the sulfuric acid content, mass ratio between polyethylene glycerol, glycerol, and peanut shell powder, liquefaction temperature, and time are 17 wt % (relative to peanut shell), 8/2/1, 150 °C, and 2 h, respectively. Furthermore, the solubility test result indicates that the liquefied products are fully soluble in the water and polyol. Meanwhile, the properties of the peanut shell and liquefaction residue were analyzed by means of attenuated total reflectance-Fourier transform infrared spectroscopy, thermal gravity analysis, and scanning electron microscope. The polysaccharide is degraded by the cleaving of C–O bond, and the lignin is decomposed by leaving the dominant linkages including β -O-4, 4-O-5, and dibenzodioxocin units. The fibers in the peanut shell are broken, and the nondegraded components in the residue lost their network structure. © 2016 Wiley Periodicals, Inc. *J. Appl. Polym. Sci.* **2016**, *133*, 44162.

KEYWORDS: cellulose and other wood products; degradation; properties and characterization; recycling

Received 26 February 2016; accepted 4 July 2016

DOI: 10.1002/app.44162

INTRODUCTION

Renewable biomass sources, such as lignocellulosics^{1–3} and other polysaccharides,⁴ are attracting considerable attention as a raw material for replacement of fossil-fuel resources. Agricultural crop wastes such as wheat straw, rice straw, cotton stalks, corn-stalks and cobs, and nut shells are abundant and renewable lignocellulosic resources in many agricultural countries, especially in Brazil, China, India, and South Africa.⁵ However, except for small amounts of them used in paper-making or biorefining industry, most of the crop wastes is abandoned or burned as fuel directly, which results in a substantial waste of lignocellulosic resources and subsequent air pollution. Consequently, the appropriate use of renewable crop wastes can reduce air pollution and improve public health and environmental quality.⁶

The crop wastes can be converted into useful products by gasification and liquefaction. Producing gas from gasification of crop waste provides a reliable, clean source of power for villages and businesses in areas that lack grid electricity. On the other hand, liquefaction is regarded as an efficient way to convert the agricultural crop wastes into useful chemical feedstock, such as bio-fuels,^{7–10} phenols and its derivatives^{11,12} and biopolyols.^{13–16}

Recent interesting in biomaterials encourage the use of the liquefied product as a renewable feedstock in manufacturing. Since agricultural crop wastes are mostly lignocellulosic biomass, which contains high content of reactive hydroxyl groups,¹⁷ the liquefied products as the biopolyols have great potential to replace petrochemical polyols for preparation of polyurethane polymers, such as adhesives,¹⁸ resins,¹⁹ and foams.¹³ In general, there are two universal approaches for liquefaction of agricultural crop wastes: (1) Liquefaction catalyzed or noncatalyzed by solvents to extract one components (cellulose, hemicellulose, or lignin) for further use.^{20–22} For example, Monteil-Rivera *et al.* have studied the extraction of lignin from triticale straw, where the ground triticale straw is liquefied by water and ethanol and catalyzed by sulfuric acid under a microwave heating. In this case, the lignin is extracted from the triticale straw and the liquefied product is not used directly but needs further treatment for removing the solvents, resulting in low overall liquefaction efficiency of the raw material. (2) Direct liquefaction without solvent recovery to produce a desirable feedstock for polymer synthesis.²³ This is an effective and promising approach to overcome the lower liquefaction efficiency of agricultural crop wastes and to further increase the ratio of biomass/

Table I. Chemical Components and Elemental Composition of the Peanut Shell

Component and element	Lignin	Holocellulose	C	H	N	O ^a
Result (wt %)	30.9	69.1	47.2	5.6	0.45	46.7

^aBy mass difference on account of only the elements of C, H, N, and O contained in the samples.

petroproducts substitution. This process makes polysaccharides (cellulose and hemicellulose) and lignin with higher molecular weight converse into lower molecular weight aromatic compounds.²⁴

The direct liquefaction processes consists of fast pyrolysis and solvolysis liquefaction. Fast pyrolysis generally involves a prompt heating of biomass to high temperatures in the absence of air,²⁵ which is the only process that is used to produce bio-oil on an industrial scale. The main product, bio-oil, is obtained in yields of up to 75 wt %.^{26,27} In comparison to fast pyrolysis, solvolysis liquefaction of biomass has more advantages. It is conducted at much lower temperature since the cellulose starts pyrolysis at as low as 150 °C. Many organic solvents, such as ethylene glycol,^{28,29} cyclic carbonates,^{29,30} or phenols,^{12,29,31} have been used for solvolysis liquefaction in the presence of strong acid or alkali. Recently, more interests have been paid on the preparation of biopolyols with polyols as solvents, where biopolyols are the renewable feedstocks for synthesis of polyurethane polymers.

In this study, therefore, as a potential approach, polyethylene glycol (PEG) and glycerol were selected as the solvents for liquefaction of the peanut shell and the reaction parameters were investigated. Furthermore, the properties of the liquefied products were also evaluated by means of solubility tests and gel permeation chromatography (GPC), and the properties of the peanut shell and liquefaction residue were characterized using different spectroscopic methods and thermal gravity (TG) analysis.

EXPERIMENTAL

Chemicals

PEG 400 is chemically pure from Tianjin Guangfu Fine Chemical Institute, China; glycerol, ethylene glycol, sulfuric acid (98.3 wt %), hydrochloric acid (36.5 wt %), *p*-toluenesulfonic acid, and sodium hydroxide are analytical grade from Yantai Sanhe Chemical Co., Ltd, Shandong, China. The peanut shell was locally collected and kindly supplied by an independent producer and originated from the cropland cultivated in Rizhao city, Shandong province, China. Washed and air-dry peanut shell samples were ground in a high-speed universal grinder (Tianjin Teste Fw80) and then sieved through a 60-mesh sieve. The peanut shell properties are listed in Table I. The percentages of carbon, hydrogen, nitrogen, and oxygen in the peanut shell were measured by an element analyzer (vario EL III; Elementar Analysensysteme GmbH).

Liquefaction of Peanut Shell

The reaction was carried out in a 250-mL three-necked flask fitted with a constantly overhead stirrer and condenser in an oil

bath. Typically, 12 g of peanut shell, 24 g of glycerol, and 96 g of PEG 400 were fed into the flask and heated to 150 °C under continuous stirring. Then 2 g of sulfuric acid was added into the flask drop by drop within 5 min. Subsequently, the temperature was kept constant at 150 °C for 2 h, after which, sodium hydroxide was added to neutralize the sulfuric acid.

Separation of Liquefied Products

The liquefied products were separated by filtration through the filter paper on a Buchner funnel under vacuum. The filter cake collected as the liquefaction residue was washed by deionized water under vacuum until the filtrate became colorless and then dried in an oven at 110 °C overnight.

The liquefaction yield is calculated as the following equation:

$$\text{liquefaction yield} = \left(1 - \frac{m_c - m_p}{m_0} \right) \times 100\% \quad (1)$$

where m_c represents the constant weight of the filter cake and the filter paper; m_p represents the constant weight of the filter paper; and m_0 represents the weight of the original peanut shell.

Characterization

The number-average molecular weight (M_n) of liquefied products was determined on a GPC system (Wyatt DAWN HELEOS II; Wyatt Technology Co., America). Polystyrene was used for the calibration curve. The mobile phase was water with a flow rate of 0.8 mL/min and an injection size of 20 mL, and the concentration of the test samples is 0.5 wt % in water.

The hydroxyl value was measured according to GB T 12008.3-2009 with a potentiometric titration method. The acid number was measured according to ASTM D7253:2006. They were conducted on an acidometer (PHS-3C; Shanghai INESA Scientific Instrument Co., Ltd) at 25 °C.

The viscosity of the liquefied product was measured at 25 °C with a rotary viscosity meter (Brookfield Programmable DV-II+ viscometer) at the rotation speed of 30 rpm.

The solubility of liquefied products was tested in different common solvents. Six drops of liquefied products were added into nine solvents (10 mL), respectively. After vigorous stirring, the blends were filtered through the filter paper to determine their solubility. Those solvents are *n*-hexane, tetrahydrofuran, ethanol, trichloromethane, methanol, deionized water, glycerol, glycerol/deionized water ($v/v = 1/1$), and methanol/deionized water ($v/v = 1/1$).

Attenuated total reflection-Fourier transform infrared (ATR-FTIR) spectra of samples were collected on an ATR-FTIR spectroscope (model VERTEX 70) in transmittance mode by means of the direct scanning. Each spectrum was recorded over 32

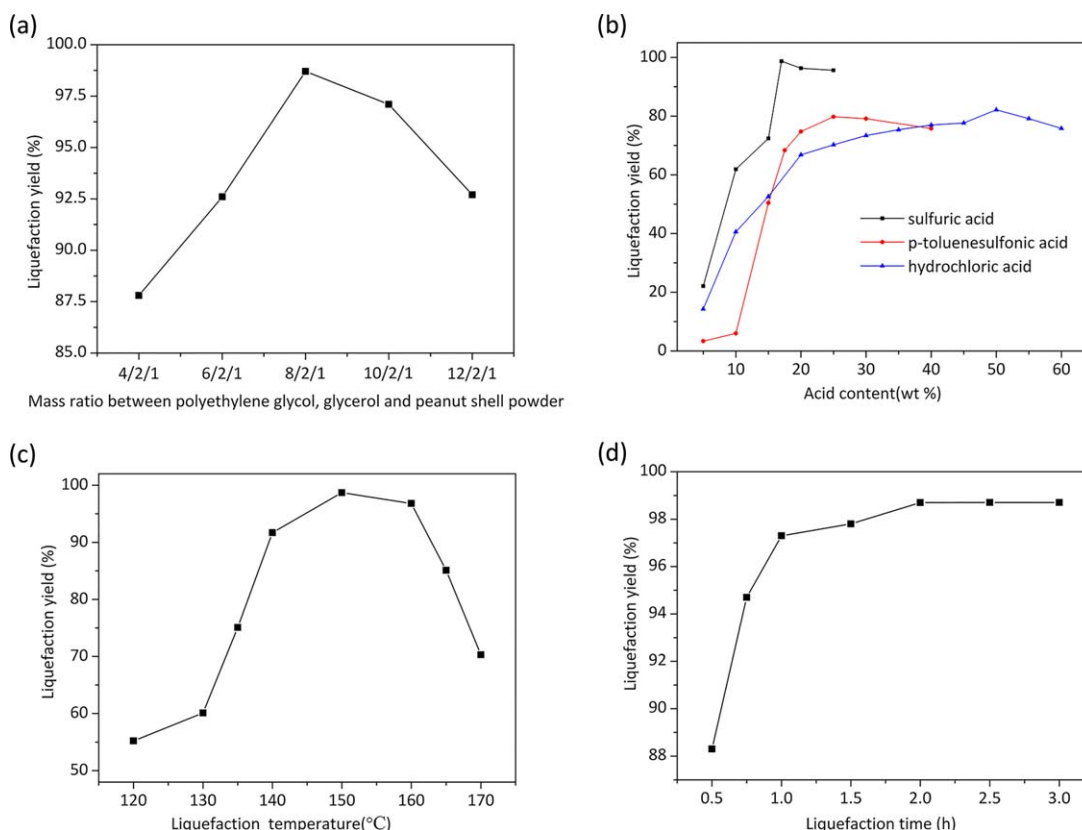


Figure 1. Liquefaction yield of peanut shell under different conditions of PEG-G-PSP ratio (a), acid type and content (relative to peanut shell) (b), liquefaction temperature (c) and time (d). Reaction conditions: (a) sulfuric acid 17%, 150 °C, 2 h, (b) PEG-G-PSP ratio 8/2/1, 150 °C, 2 h, (c) PEG-G-PSP ratio 8/2/1, sulfuric acid 17%, 2 h, and (d) PEG-G-PSP ratio 8/2/1, sulfuric acid 17%, 150 °C. [Color figure can be viewed in the online issue, which is available at wileyonlinelibrary.com.]

scans in the range from 4000 to 600/cm, with a resolution of 2/cm.

Thermal degradation of the samples was studied via TG analysis, which was carried out in a NETZSCH TG 209 F1 thermogravimetric analyzer. The samples of 3–5 mg were heated from room temperature up to 800 °C at a rate of 10 °C/min with a nitrogen flow of 40 mL/min as purge gas.

The pore microstructure of the samples was observed on a cold-field emission scanning electron microscope (SEM; Hitachi S-4800) equipped with a backscattered electron detector operating at 3 kV. Samples were observed under the same degree of magnification of $\times 30$ using a Charge Reduction Sample Holder.

RESULTS AND DISCUSSION

Effect of Liquefaction Conditions

PEG 400, glycerol, ethylene glycol, and the mixture of PEG 400 and glycerol (PEG-G) and the mixture of PEG 400 and ethylene glycol (PEG-EG) were selected to examine the influence of solvents on the liquefaction efficiency. It is found that the highest liquefaction yield of 98.7 wt % could be achieved in PEG-G solvent, since the liquefied products have the similar structure with PEG and the solubility of liquefied products can be further improved by addition of the glycerol. Therefore, the PEG-G was chosen as the solvent in the following experiments.

The mass ratio between polyethylene glycol, glycerol, and peanut shell powder is defined as PEG-G-PSP ratio in the following text. The experimental results for liquefaction yield under different conditions of PEG-G-PSP ratio, acid type and content (relative to peanut shell), liquefaction temperature and time are shown in Figure 1. As can be seen in Figure 1(a), the liquefaction yield increases at lower PEG-G-PSP ratio, reaches to maximum value of 98.7%, and then decreases with further increase in PEG-G-PSP ratio. This may be explained as follows. At lower PEG-G-PSP ratio, the sulfuric acid has a relative higher concentration in the reaction matrix, resulting in dehydration and carbonization of liquefied product. However, as the PEG-G-PSP ratio is further increased, the sulfuric acid content becomes too low in reaction matrix so that it is unable to play the same catalytic role as the PEG-G-PSP ratio of 8/2/1. As a result, the liquefaction yield is reduced.

The degradation of lignocellulosic biomass using organic solvents during liquefaction proceeds is mainly hydrolysis and solvolysis processes,² in which the liquefaction efficiency can be improved by acids catalyst.³² In the liquefaction, acid as catalyst accelerates not only the degradation of biomass in the earlier stage but also the recondensation of fragments in the later stage.³³ In this study, sulfuric acid, hydrochloric acid and *p*-toluenesulfonic acid, were selected as catalysts during liquefaction process. As show in Figure 1(b), among the three kinds of acid

Table II. Physicochemical Properties of Liquefied Product and Solvents

Physicochemical properties	Hydroxyl number (mg KOH g ⁻¹)	Acid number (mg KOH g ⁻¹)	Viscosity (MPa s, 25 °C)	Molecular weight (g mol ⁻¹)	Color
Liquefied product	451.91	8.92	47	312.5	Black
PEG-G	337.06	0.1	41	329.4	Colorless

catalysts, the sulfuric acid exhibited preferable catalytic efficiency at low catalyst content. Typically, it is found that the liquefaction yield shows an increase of more than 95% at the sulfuric acid content of 17–25% (relative to peanut shell powder). However, the liquefaction yield is only between 50% and 80% with the same content of hydrochloric acid or *p*-toluene-sulfonic acid. This can be attributed to the high catalytic activity and dehydration of sulfuric acid with low content in early reaction stage of alcoholysis.³⁴ It should be noted that the excessive amounts of sulfuric acid with strong oxidizability need the anticorrosion reactor. Therefore, 17% sulfuric acid catalyst is recommended on the actual production.

Figure 1(c,d) shows the influence of reaction temperature and time on the liquefaction yield. It can be seen that the liquefaction yield increases with temperatures at lower temperature due to the decomposition of peanut shell into intermediates compounds with small molecular, then reaches to a maximum value at the temperature of 150 °C. As the temperature is further increased, the liquified product would be converted into residue through annulation and repolymerization reaction, resulting in a reduction in liquefaction yield. This is consistent with the report from previous study 35. In the case of reaction time in Figure 1(d), liquefaction yield reaches a plateau after a sharp increase with time. This indicates the liquefaction reaction is completed in very short time, even less than 2 h.

GPC Characterization of Liquefied Products

The liquefied product was obtained at a PEG-G-PSP ratio of 8/2/1, sulfuric acid content of 17%, temperature of 150 °C, and reaction time of 2 h. In this case, the M_n of liquefied products and PEG-G solvent is 312.5 and 329.4 g/mol, respectively. It indicates that the M_n of liquefied products is close to that of PEG-G solvent. The liquefied product with low molecular weights is suitable for preparing the rigid polyurethane foams (generally M_n between 300 and 400 g/mol),³⁷ due to the improvement of cross-linking density in synthesis process.

Acid Number and Hydroxyl Number Characterization of Liquefied Products

The acid number and hydroxyl number were measured over the final liquefied product obtained under the optimum liquefaction condition of the PEG-G-PSP ratio of 8/2/1, sulfuric acid content of 17%, temperature of 150 °C, and reaction time of 2 h. As seen in Table II, the acid number of the liquefaction solvent at the beginning of the liquefaction reaction was measured to be approximate 0.1 mg KOH/g. The value increased to 8.92 mg KOH/g at the time of 2 h. The addition of acidic substances in the reaction system and the oxidation of the cellulose, hemicellulose and lignin caused the increase of acid number during the liquefaction.³⁷

It can be seen from the hydroxyl number tests that the hydroxyl number increase dramatically from approximate 337.06 mg KOH/g of solvents to 451.91 mg KOH/g of final liquefied products. And generally, the appropriate hydroxyl number for rigid polyurethane preparation is 200–550 mg KOH/g.³⁶ Therefore, the test results indicate that the liquefied products contain abundant hydroxyl from cellulose, hemicellulose, and lignin of peanut shell and can be utilized as polyol for preparing rigid polyurethane foams.

Viscosity Characterization of Liquefied Products

Table II shows that the viscosity of liquefied products is 47 mPa s at 25 °C; it is close to the viscosity of 41 mPa s of PEG-400. The viscosity of liquefied products was found to depend on the liquefying solvents. Thus, the viscosity is feasible condition for preparation of rigid polyurethane foams.

Solubility Tests of Liquefied Products

The lignocellulosics always have poor solubility in common solvents due to their complicated three-dimensional lignin network in the peanut shell interlinked with polysaccharide components to form the entire peanut shell matrix. As a result, the insolubility of lignocellulosics in common solvents prevents them from reacting with other materials. In this work, the solubility of lignocellulosics has been substantially improved via liquefaction process, where lignin and polysaccharide in lignocellulosics were decomposed into components with smaller molecular weight such as sugar derivatives and phenolics.

It can be seen from Table III and Figure 2, the liquefied products can be totally dissolved in deionized water and PEG. However, the peanut shell powder is completely insoluble in these solvents, since the liquefied products of the peanut shell has the similar structure to the PEG. These results indicate that it is

Table III. The Solubility of Liquefied Products in the Common Solvents

Solvents	Solubility
<i>n</i> -Hexane	Insoluble
Tetrahydrofuran	Partly soluble
Ethanol	Partly soluble
Trichloromethane	Partly soluble
Glycerol	Partly soluble
Methanol	Mostly soluble
Glycerol/deionized water($v/v = 1/1$)	Mostly soluble
Methanol/deionized water($v/v = 1/1$)	Mostly soluble
Deionized water	Totally soluble
Polyethylene glycol	Totally soluble

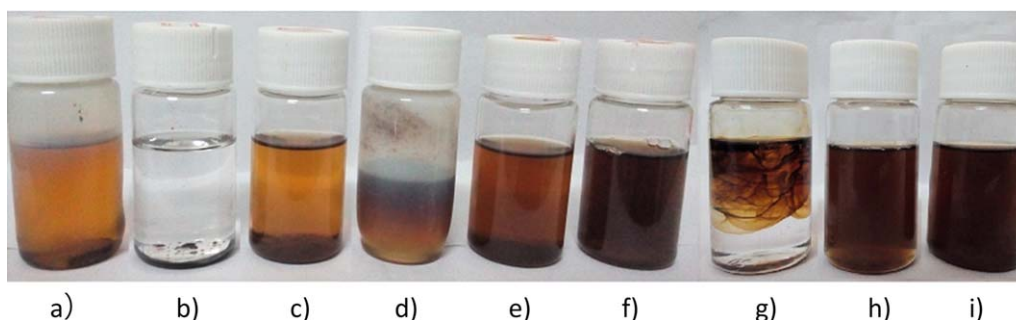


Figure 2. The solubility of liquefied products in the common solvents; (a) tetrahydrofuran, (b) n-Hexane, (c) ethanol, (d) trichloromethane, (e) methanol, (f) deionized water, (g) glycerol, (h) glycerol/deionized water ($v/v = 1/1$), (i) methanol/deionized water ($v/v = 1/1$). The liquefied products was synthesized at a PEG-G-PSP ratio of 8/2/1, sulfuric acid content of 17%, temperature of 150°C, and reaction time of 2 h. [Color figure can be viewed in the online issue, which is available at wileyonlinelibrary.com.]

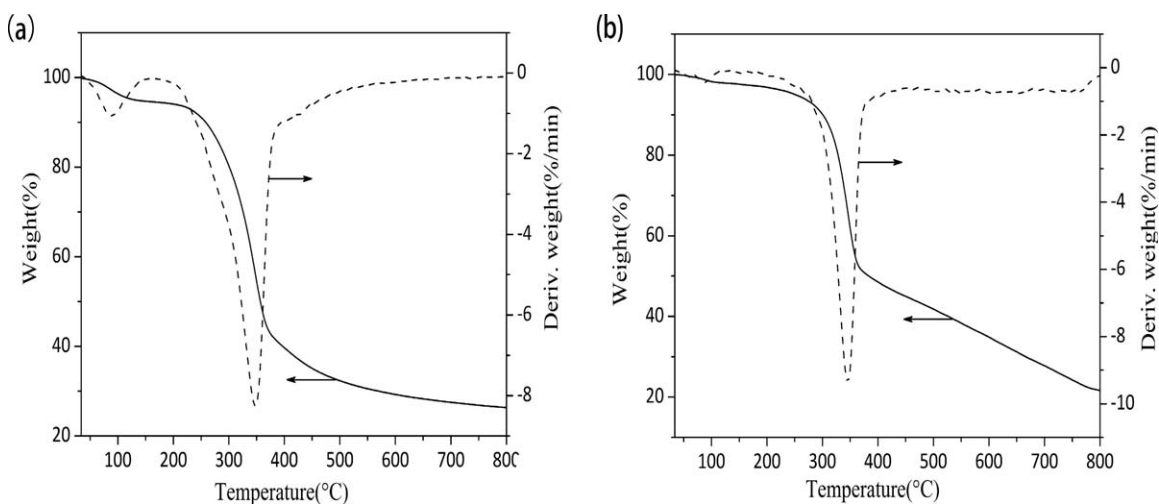


Figure 3. Thermogravimetric and derivative thermogravimetric curves of the peanut shell (a) and liquefaction residue (b) under a N_2 atmosphere. The residue was obtained at a reaction condition of PEG-G-PSP ratio 8/2/1, sulfuric acid 17%, 150°C, and 2 h.

more preferable for liquefied products to replace the petrochemical polyols to react with the diisocyanate forming the polyurethane materials because they have only minor steric hindrance compared with lignocellulosics. Furthermore, the products are mostly soluble in methanol, glycerol/deionized water ($v/v = 1/1$) and methanol/deionized water ($v/v = 1/1$), while only partly soluble in ethanol, glycerol, tetrahydrofuran, and trichloromethane. This can also be explained as the solubility of the liquefied products depending on the polarity of the solvent. Therefore, the liquefied products are fully soluble in the water and polyol with strong polarity and totally insoluble in the non-polar solvent such as n-hexane.

TG Analysis of the Peanut Shell and Liquefaction Residue

Figure 3 exhibits the TG and derivate thermogravimetric curves of peanut shell and liquefaction residue in a N_2 atmosphere. The specific degradation temperatures, maximum degradation temperature, and final char yield at 800°C are summarized in Table IV. T_{max} is defined as the maximum degradation temperature.

The degradation of peanut shell often starts at the hemicellulose, followed by cellulose and lignin.³⁸ As can be seen in Figure 3 and Table IV, the temperature at the maximal rate of weight loss is 348°C from peanut shell curve similar to that of liquefaction residue. However, temperatures at weight loss of 5% and

Table IV. Thermogravimetric and Derivative Thermogravimetric Analysis Data of Peanut Shell and Liquefaction Residue

Sample	Temperature at weight loss of 5% (°C)	Temperature at weight loss of 50% (°C)	T_{max} (°C)	Char (wt %, 800 °C)
Peanut shell	130.5	356.5	348	26.3
Liquefaction residue	250	383	345	21.7

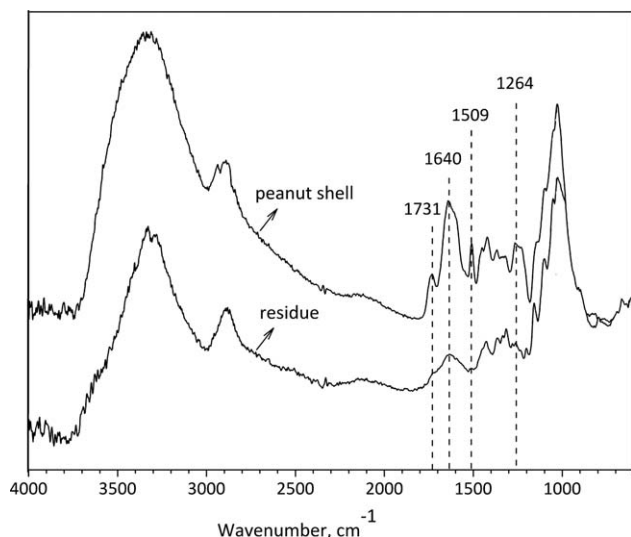


Figure 4. ATR-FTIR spectra of peanut shell and residue. The residue was obtained at a reaction condition of PEG-G-PSP ratio 8/2/1, sulfuric acid 17%, 150 °C, and 2 h.

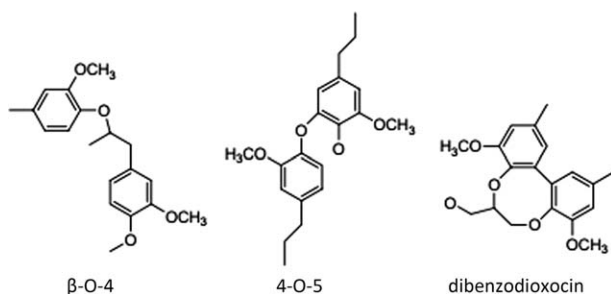


Figure 5. Lignin linkages including β -O-4, 4-O-5, and dibenzodioxocin.⁴² Reaction conditions: PEG-G-PSP ratio 8/2/1, sulfuric acid 17%, 150 °C, and 2 h.

50% for liquefaction residue are around 250 and 383 °C, respectively, higher than that of peanut shell about 130.5 and 356.5 °C, and the final char of liquefaction residue is 21.7%

lower than that of peanut shell about 26.3%. These results indicate that the liquefaction residue shows inferior thermal stability as compared to the peanut shell, since the liquefaction residue was the degradation product from the peanut shell.

ATR-FTIR characterization of the Peanut Shell and Liquefaction Residue

FTIR spectrum of the lignocellulosic biomass is usually complicated due to versatile functional groups contained in the lignin and polysaccharide. A great many of peaks in FTIR spectra of the lignocellulosic biomass stretch a wide range and frequently overlap with the nearby peaks. As shown in Figure 4, the majority of frequency vibration for peanut shell and residue are detected in the similar position. A broad peak at around 3329/cm arises from the OH stretching vibration either from phenolic hydroxyl group of lignin or alcoholic hydroxyl group of polysaccharide.³⁹ The peak at 2882/cm is assigned to the C—H stretching vibration in methyl and methylene groups.

An absorbance at approximate 1731/cm can be seen in spectrum of the peanut shell whereas it becomes very weak or even disappeared in the spectrum of residue. Typically, the absorption band at 1731/cm corresponds to the C=O stretching vibration in carboxylic or ester group from polysaccharide and the non-conjugated beta carbonyl group from lignin.⁴⁰ It indicates that the liquefaction treatment leads to degradation of peanut shell, which can be interpreted as the alcoholysis of the ester linkages in the xylan in the presence of the sulfuric acid. The residue not only consists of degradation products but contains persistent components with larger molecules which are hard to dissolve in the PEG-G solvent via alcoholysis. Contrarily, the liquefied components undergo a further degradation to generate small molecules which can integrate with the polyhydric alcohols. Furthermore, xylan is one of the major hemicelluloses present in plant cell wall matrix, where it is closely associated with other cell wall constituents, such as lignin and pectic polysaccharides, by ferulic acid or uronic acid through ester linkages.³⁰

Bands at around 1640 and 1509/cm are characteristic peaks of the C=C stretching vibration in the aromatic skeleton of

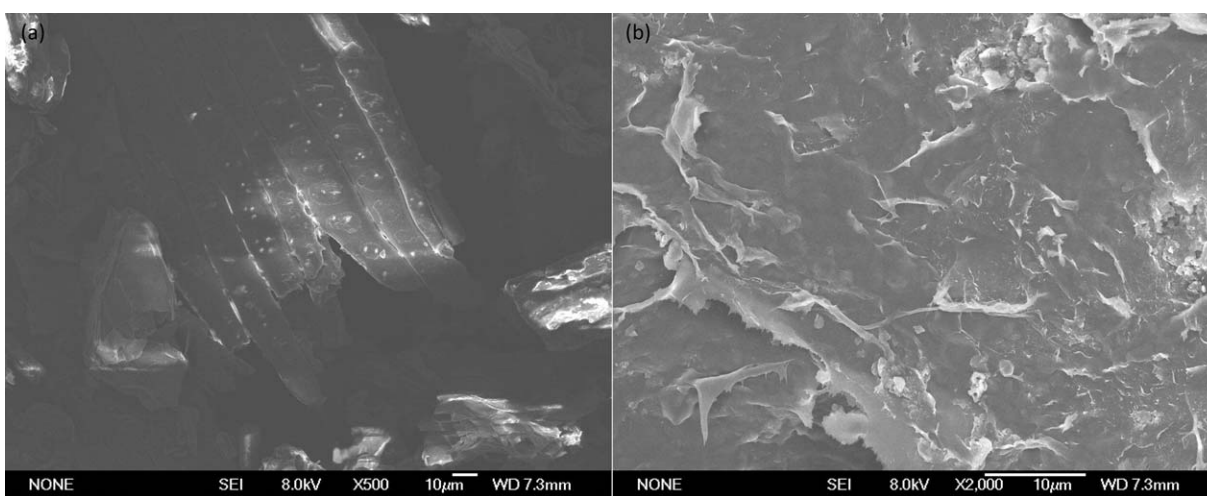


Figure 6. SEM images of peanut shell (a) and liquefaction residue (b). The residue was obtained at a reaction condition of PEG-G-PSP ratio 8/2/1, sulfuric acid 17%, 150 °C, and 2 h.

lignin.^{24,39} Compared to the peanut shell spectrum, the absorption band at 1640/cm becomes weaker, and the band at 1509/cm almost disappears in the residue spectrum, indicating that the lignin had been significantly degraded under optimum liquefaction conditions. The absorbance at 1264/cm, which is due to C—O—C stretching vibration in β -glucosidic bonds of polysaccharide and the characteristic absorbance in guaiacyl (G) alcohol units of lignin, becomes very weaker on residue spectrum. This shows that the polysaccharide is degraded by the cleaving the C—O bond, and the lignin is decomposed by leaving the dominant linkages including β -O—4, 4—O—5, and dibenzodioxocin units (see Figure 5), as reported by previous study.^{41,42}

SEM of the Peanut Shell and Liquefaction Residue

The SEM images of peanut shell powder and the liquefaction residue are presented in Figure 6. It is observed that the raw material contains the aligned fibrous components with uniform size, whereas the residue only consists of the lacerated flocculate. This indicates the fibers in the peanut shell are broken, and the nondegraded components in the residue lost the network structure, while the degraded segments fall off from the original fiber structure.

CONCLUSIONS

This work has demonstrated a simple and highly efficient process for liquefying the peanut shell. And the liquefied products can be used directly to prepare the polyurethane materials. Compared to single-solvent, the mixture of PEG and glycerol as solvents showed higher liquefaction efficiency for the liquefaction of peanut shell with the sulfuric acid as a catalyst. And the preferable maximum liquefaction yield of 98.7 wt % could be achieved when the sulfuric acid content, PEG-G-PSP ratio, liquefaction temperature, and time are 17 wt % (relative to peanut shell), 8/2/1, 150 °C, and 2 h, respectively. Solubility tests show that the solubility of liquefied products is dependent on the polarity of the solvents, and the liquefied products can be totally dissolved in deionized water and PEG, completely insoluble in nonpolar solvent. GPC suggests that the liquefied products are preferable for preparing the rigid polyurethane foams. ATR-FTIR shows that the polysaccharide is degraded by the cleaving the C—O bond, and the lignin is decomposed by leaving the dominant linkages including β -O—4, 4—O—5, and dibenzodioxocin units. TG analysis demonstrates that the liquefaction residue shows inferior thermal stability than the peanut shell. SEM analysis indicates the fibers in the peanut shell are broken and the non-degraded components in the residue lost the network structure, while the degraded segments come off from the original fiber structure. And this liquefaction process provides a potential approach to generate high-quality chemical feedstocks, which can be used directly to prepare rigid polyurethane foams without solvents recovery.

ACKNOWLEDGMENTS

This project was supported by the National Natural Science Foundation of China (grant number U1510109) and Start-up Foundation of Qingdao University of Science and Technology.

REFERENCES

- Sequeiros, A.; Serrano, L.; Briones, R.; Labidi, J. *J. Appl. Polym. Sci.* **2013**, *130*, 3292.
- Hassan, EbM.; Shukry, N. *Ind. Crop. Prod.* **2008**, *27*, 33.
- Wang, Z.; Xu, S.; Hu, W. P.; Xie, Y. *J. BioEnergy Res.* **2013**, *6*, 896.
- Baruque, F. E. A.; Baruque, M. D. G. A.; Sant'Anna, G. L. *Bioresour. Technol.* **2000**, *75*, 49.
- Arnal, E.; Förster, M. Tackling Inequalities in Brazil, China, India and South Africa: The Role of Labour Market and Social Policies; OECD publishing: Paris, **2010**; p 13.
- Ahiduzzaman, M.; Islam, A. K. M. A.; Yaakob, Z.; Ghani, J. A.; Anuar, N. Agricultural Residues from Crop Harvesting and Processing: A Renewable Source of Bio-Energy; Springer International Publishing: Berlin, **2014**; p 323.
- Maksoud, A.; Cui, L.; Hu, H. W.; Shields, J. *Green Chem.* **2014**, *16*, 3031.
- Chen, F.; Dixon, R. A. *Nat. Biotechnol.* **2007**, *25*, 759.
- Chuck, C. J.; Parker, H. J.; Jenkins, R. W.; Donnelly, J. *Bioresour. Technol.* **2013**, *143*, 549.
- Ciesielski, P. N.; Resch, M. G.; Hewetson, B.; Killgore, J. P.; Curtin, A.; Anderson, N.; Chiaramonti, A. N.; Hurley, D. C.; Sanders, A.; Himmel, M. E.; Chapple, C.; Mosier, N.; Donohoe, B. S. *Green Chem.* **2014**, *16*, 2627.
- Karagöz, S.; Bhaskar, T.; Muto, A.; Sakata, Y. *Fuel* **2004**, *83*, 2293.
- Tymchyshyn, M.; Xu, C. C. *Bioresour. Technol.* **2010**, *101*, 2483.
- Hu, S. J.; Wan, C. X.; Li, Y. B. *Bioresour. Technol.* **2012**, *103*, 227.
- Luo, X. L.; Hu, S. J.; Zhang, X.; Li, Y. B. *Bioresour. Technol.* **2013**, *139*, 323.
- Matos, M.; Barreiro, M. F.; Gandini, A. *Ind. Crop. Prod.* **2010**, *32*, 7.
- Zhang, T.; Zhou, Y.; Liu, D.; Petrus, L. *Bioresour. Technol.* **2007**, *98*, 1454.
- Sanghamitra, S.; Hasan, S.; Argyropoulos, D. S. *Biomacromolecules* **2013**, *14*, 3399.
- Lee, W. J.; Lin, M. S. *J. Appl. Polym. Sci.* **2008**, *109*, 23.
- Wei, Y. P.; Cheng, F.; Li, H. P.; Yu, J. G. *J. Appl. Polym. Sci.* **2004**, *92*, 351.
- Monteil-Rivera, F.; Huang, G. H.; Paquet, L.; Deschamps, S.; Beaulieu, C.; Hawari, J. *Bioresour. Technol.* **2012**, *104*, 775.
- Monteil-Rivera, F.; Phuong, M.; Ye, M.; Halasz, A.; Hawari, J. *Ind. Crop. Prod.* **2013**, *41*, 356.
- Vanderlaan, M. N.; Thring, R. W. *Biomass Bioenergy* **1998**, *14*, 525.
- Fan, S. P.; Zakaria, S.; Chia, C. H.; Jamaluddin, F.; Nabihah, S.; Liew, T. K.; Pua, F. L. *Bioresour. Technol.* **2011**, *102*, 3521.
- Xu, J. M.; Jiang, J. C.; Hse, C. Y.; Shupe, T. E. *Green Chem.* **2012**, *14*, 2821.
- Lu, Q.; Yang, X. C.; Dong, C. Q.; Zhang, Z. F.; Zhang, X. M.; Zhu, X. F. *J. Anal. Appl. Pyrol.* **2011**, *92*, 430.
- Bridgwater, A. V. *Biomass Bioenergy* **2012**, *38*, 68.

27. Czernik, S.; Bridgwater, A. V. *Energy Fuel* **2004**, *18*, 590.
28. Rezzoug, S. A.; Capart, R. *Appl. Energy* **2002**, *72*, 631.
29. Yip, J.; Chen, M.; Szeto, Y. S.; Yan, S. *Bioresour. Technol.* **2009**, *100*, 6674.
30. Yamadaa, T.; Ono, H. *Bioresour. Technol.* **1999**, *70*, 61.
31. Mishra, G.; Saka, S. *Bioresour. Technol.* **2011**, *102*, 10946.
32. Wang, H.; Chen, H. Z. *J. Chin. Inst. Chem. Eng.* **2007**, *38*, 95.
33. Ge, J. J.; Wu, R.; Deng, B. L.; Shi, X. H.; Wang, M.; Li, W. J. *Sci. Eng.* **2003**, *19*, 194.
34. Chen, F. G.; Lu, Z. M. *J. Appl. Polym. Sci.* **2009**, *111*, 508.
35. Pawlik, H.; Prociak, A. *J. Polym. Environ.* **2012**, *20*, 438.
36. Liu, Y. J. In *Handbook of Raw Materials and Additives for Polyurethanes*; Chemical Industry Press: Beijing, **2012**; p 71; Chapter 2.
37. Pu, S.; Shiraishi, N. *Mokuzai Gakkaishi* **1994**, *40*, 824.
38. Pan, H.; Shupe, T. F.; Hse, C. Y. *J. Appl. Polym. Sci.* **2007**, *105*, 3739.
39. Hoareau, W.; Trindade, W. G.; Siegmund, B.; Castellan, A.; Frohini, E. *Polym. Degrad. Stabil.* **2004**, *86*, 567.
40. Souza, A. P. D.; Leite, D. C. C.; Pattathil, S.; Hahn, M. G.; Buckeridge, M. S. *Bioenergy Res.* **2012**, *6*, 564.
41. Huber, G. W.; Iborra, S.; Corma, A. *Chem. Rev.* **2006**, *106*, 4044.
42. Chakar, F. S.; Ragauskas, A. *J. Ind. Crop. Prod.* **2004**, *20*, 131.